Eur. J. Biochem. *250*, 524−531 (1997)

Molybdate-uptake genes and molybdopterin-biosynthesis genes on a bacterial plasmid

Characterization of MoeA as a filament-forming protein with adenosinetriphosphatase activity

Cástor MENÉNDEZ[1], Annegret OTTO[1], Gabor IGLOI[2], Peter NICK[2], Rainer BRANDSCH[3], Berthold SCHUBACH[4], Bettina BÖTTCHER[4] and Roderich BRANDSCH[1]

[1] Institut für Biochemie und Molekularbiologie, Universität Freiburg, Germany
[2] Institut für Biologie III, Universität Freiburg, Germany
[3] Institut für Materialforschung, Universität Freiburg, Germany
[4] Insitut für Physikalische Chemie, Universität Freiburg, Freiburg, Germany

(Received 13 August/13 October 1997) − EJB 97 1170/2

A gene cluster consisting of homologs to *Escherichia coli moaA*, *moeA*, *moaC* and *moaE*, which encode enzymes involved in the biosynthesis of molybdopterin cofactor (MoCo), and to *modA*, *modB* and *modC*, which encode a high-affinity molybdate transporter, were identified on pAO1 of *Arthrobacter nicotinovorans* near genes of molybdopterin-dependent enzymes involved in nicotine degradation. This gene arrangement suggests a coordinated expression of the MoCo-dependent and the MoCo-biosynthesis genes and shows that catabolic plasmids may carry the transport and biosynthetic machinery for the synthesis of the cofactors needed for the functioning of the enzymes they encode. pAO1 MoeA functionally complemented *E. coli moeA* mutants. The overexpressed and purified protein, of molecular mass 44 500 Da, associated into high-molecular-mass complexes and spontaneously formed gels at concentrations above 1 mg/ml. Transmission electron microscopy and atomic force microscopy revealed that MoeA forms fibrilar structures. In the presence of Mg^{2+} MoeA exhibited ATPase activity (0.020 pmol ATP · pmol protein^{-1} · min^{-1}). ATP, ADP or AMP induced the disassembly of the MoeA fibers into aggregates. pAO1 MoeA shows 39% identity to the C-terminal domain of the rat neuroprotein gephyrin. Like gephyrin it binds to neurotubulin, but binds with preference to tubulin dimers.

Keywords: catabolic-enzyme-encoding plasmid; MoeA; molybdopterin cofactor; molybdenum-containing enzyme; Mg^{2+}-ATPase.

Molybdopterin is the common cofactor of a large group of molybdenum enzymes, which play essential roles from bacteria to man. Its synthesis involves many gene products, generically called Mol, many of which are conserved in all living organisms but only a few have been defined functionally (Rajagopalan and Johnson, 1992). The biochemical activities of MoaA, MoaB, MoaC and MoeA are unknown; genetic studies suggest, however, that these gene products may be involved in the first biosynthetic steps leading to a precursor molecule (precursor Z) of the molybdopterin cofactor (MoCo). MoeA shows significant similarity to eukaryotic proteins, such as the cinnamon gene product of *Drosophila melanogaster*, the N-terminus of Cnx1 from *Arabidopsis thaliana*, gephyrin from *Rattus norwegigus*, and a gene product of *Caenorhabditis elegans*. The N-termini of cinnamon and gephyrin are similar to MoaB and MogA, proteins with unknown functions in MoCo synthesis, but which are known to bind molybdate (Kamdar et al., 1994). Bacterial uptake of molybdate is performed by a high-affinity Mo transporter of the ATP-binding-cassette type, typically consisting of a periplasmic Mo-binding protein, ModA, a membrane pore formed by a dimer of ModB, and a membrane-associated ATP-binding dimeric protein representing the energizer of the uptake system, ModC (Higgins, 1992).

Soil bacteria make use of plasmids to carry inducible genes of catabolic enzymes, which enable them to use a large variety of organic substrates, when present in the medium, as a source of energy. The cofactors needed for holoenzyme formation and thus enzyme activity are assumed to be supplied by the activity of chromosomally encoded biosynthetic enzymes. The ability of *Arthrobacter nicotinovorans* to grow on the tobacco alkaloid nicotine (Eberwein et al., 1961) is linked to the presence of the 160-kb catabolic plasmid pAO1 in the bacterial cells (Bernauer et al., 1992). Nicotine dehydrogenase, the first enzyme of the degradative pathway (Grether-Beck et al., 1994), a heterotrimeric protein complex, belongs to a class of bacterial hydroxylases of similar structure that contain as cofactors [2Fe-2S] clusters, FAD and MoCo in its dinucleotide form (Kretzer et al., 1993). We have shown previously that a copy of a *moaA* gene is located close to the *ndh* genes on pAO1 (Menéndez et al., 1995, 1996). Here we show that *moaA* of pAO1 belongs to a

Correspondence to R. Brandsch, Institut für Biochemie und Molekularbiologie, Hermann-Herder-Strasse 7, D-79104 Freiburg i. Br., Germany
Fax: +49 761 203 5253.
E-mail: brandsch@ruf.uni-freiburg.de

Abbreviations. MoCo, molybdopterin cofactor; TEM, transmission electron microscopy; AFM, atomic force microscopy.

Note. The nucleotide sequence data presented here have been deposited with the EMBL database and are available under the accession number Y10817.

Table 1. Bacterial strains and plasmids.

Bacterial strain/ plasmid	Genotype/relevant marker	Reference/source
E. coli JM109	e14-(*mcrA*), *recA1, endA1, gyrA96, thi-1, hsdR17* (rk^-, mk^+), *supE44, relA1,* D(*lac-proAB*), [F′ *traD36, proAB, lac*$I^qZ\Delta$M15]	Yanish-Peron et al. (1985)
E. coli RK4353	*araD139 Δ(argF-lac) U169 deoC1 flhD5301 gyrA219 non-9 ptsF25 relA1 rpsL150*	Stewart and McGregor (1982)
E. coli RK5201	As RK4353 but *moeA201*:: Muc^{ts}	
E. coli RK5202	As RK4353 but *modC202*:: Muc^{ts}	
A. nicotinovorans	$pAO1^+/Nic^+$	Eberwein et al. (1961)
pBluescriptKS II^-	Amp^r, T3/T7 promoters, cloning vector	Stratagene
pH6EX3	Amp^r, *lac*I^q, p_{tac}, His_6 fusion, expression vector	Berthold et al. (1992)
pNG0201	Amp^r, p_{tac}, *ndhABC, moaA*, IS1473, 7.1-kb *Eco*RI−*Eco*RI pAO1 DNA in pKK223-3	Grether-Beck et al. (1994)
pCM2218	*mol* cluster, 10.8-kb *Hin*dIII−*Spe*I pAO1 DNA in pBS	this work
pCM2219	*moeA, moaC, moaE, modA*, 4.1-kb *Eco*RI−*Eco*RI DNA in pBS	
pCM2221	*modC* and *bgx*A, 5.1-kb *Eco*RI−*Cla*I pAO1 DNA in pBS	
pBS-moeA	*moeA*, 1.4 kb *Hin*dIII−*Stu*I pAO1 DNA in pBS	
pBS-moaA	*moaA*, 1.6 kb *Hin*dIII−*Spe*I pAO1 DNA in pBS	
p6H-MoeA	His_6 fusion, 1.3-kb *Bam*HI−*Stu*I in pH6EX3	
p6H-MoaC	His_6 fusion, 700-bp *Bam*HI−*Eco*RI in pH6EX3	
p6H-MoaE	His_6 fusion, 500-bp *Bam*HI−*Eco*RI in pH6EX3	

mol-gene cluster consisting of *moeA*, *moaC*, *moaE* and the *modABC* genes of a high-affinity molybdate transporter- with *moaA* transcribed divergently to the rest of the *mol* genes. The assembly of genes encoding MoCo-dependent enzymes and genes encoding enzymes of MoCo synthesis and Mo uptake on a catabolic plasmid may reflect the formation of a functional unit aimed at the coordination of the synthesis of the apoenzymes and the synthesis of the molybdopterin cofactor.

The gene product of pAO1 *moeA* has been overexpressed and purified. Its biochemical characterization revealed unexpected features of the MoeA protein, which are presented in this work.

MATERIALS AND METHODS

Chemicals and biochemicals. All chemicals used were of highest purity available. Isopropylthio-*β*-galactoside, 5-bromo-4-chloro-3-indolyl-*β*-D-galactopyranoside and thrombin were from Sigma. Restriction endonucleases were from New England Biolabs or MBI-Fermentas. DNA polymerase I, Klenow fragment, T7 and T3 RNA polymerases, T4 ligase and alkaline phosphatase were from Boehringer Mannheim, Taq DNA polymerase was from Pharmacia. α-^{32}P-labeled nucleoside triphosphates and [^{35}S]methionine were from Amersham Buchler.

Bacterial strains and culture conditions. The strains and plasmids used in this work are listed in Table 1. Bacteria were grown in Luria-Bertani medium (Sambrook et al., 1989) and cell extracts were prepared from bacterial pellets of overnight cultures as described (Bernauer et al., 1992). Functional complementation of *E. coli* mutant strains deficient in Mol activity with the corresponding pAO1 genes was performed by the nitrate reductase activity test on agar plates as described previously (Menéndez et al., 1995). M9 defined mineral medium was used in complementation tests with *E. coli* mutants in Mo transport. Induction of the bacterial production, and affinity purification of the His_6-fusion protein was performed as described (Berthold et al., 1992).

Recombinant DNA techniques. Isolated pAO1 DNA (Menéndez et al., 1997) was digested with a combination of *Hin*dIII and *Spe*I restriction enzymes and the DNA fragments obtained were cloned into the vector pBluescript KSII. *E. coli* transformants carrying the region upstream of *moaA* were identified by colony hybridization with a *moaA* [^{32}P]DNA probe labeled by random primer transcription of the *moaA* gene cloned in plasmid pNG0201 (Menéndez et al., 1995). Subcloning of DNA fragments from pCM2218 carrying individual genes into pBluescript KSII and pH6EX3 (Table 1) was performed by standard methods (Sambrook et al., 1989).

DNA sequencing and analysis. DNA sequencing was performed on both strands with fluorescent oligonucleotides. The presence of potentially coding ORF was evaluated with the program NuclPepSearch (Gonnet et al., 1992). Database similarity searches coupled to potential domains and motifs searches were done using the Beauty server (Worley et al., 1995) and the Prosite database (Bairoch et al., 1995).

Overexpression and purification of pAO1 MoeA in *E. coli*. *E. coli* cells carrying the recombinant plasmid p6H-MoeA (Table 1) were induced with 1 mM isopropylthio-*β*-galactoside at 24°C for 24 h. The cells were sonified, centrifuged, and the soluble fraction passed through a Ni^{2+}-chelate affinity column. The MoeA protein bound to the affinity material was eluted with a gradient of imidazole. The elution of the protein was monitored by SDS/PAGE. When required, the His_6 tag was removed from the fusion protein by digestion with thrombin.

PAGE and molecular-sieve chromatography. MoeA was analysed by SDS/PAGE and native PAGE according to standard procedures (Sambrook et al., 1989). Cross-linking of MoeA was performed in 15-µl assays containing 10 µg MoeA in 1 M sodium borate, pH 8.5, by the addition of 1.5 µl 0.2 M glutaraldehyde. Reactions were stopped after 30 s by the addition of 1.5 µl 1 M $NaBH_4$ and run on SDS/PAGE. Molecular-sieve chromatography was performed on Superdex 200.

Measurement of nucleotide triphosphate hydrolysis. The nucleotide triphosphate hydrolytic activity of MoeA was determined by TLC. Standard assay conditions consisted of 3.3 pmol [α-^{32}P]NTP (3000 Ci/mmol) in 20 µl 10 mM Tris/HCl pH 7.5, 10 mM $MgCl_2$ and various additions of MoeA, incubated at 30 °C for different times. 2 µl of the reaction mixture were spotted on polyethyleneimine-impregnated cellulose plates (Machery-Nagel), chromatographed with 0.5 M formic acid, 0.5 M LiCl for 45 min, and the plates autoradiographed. The

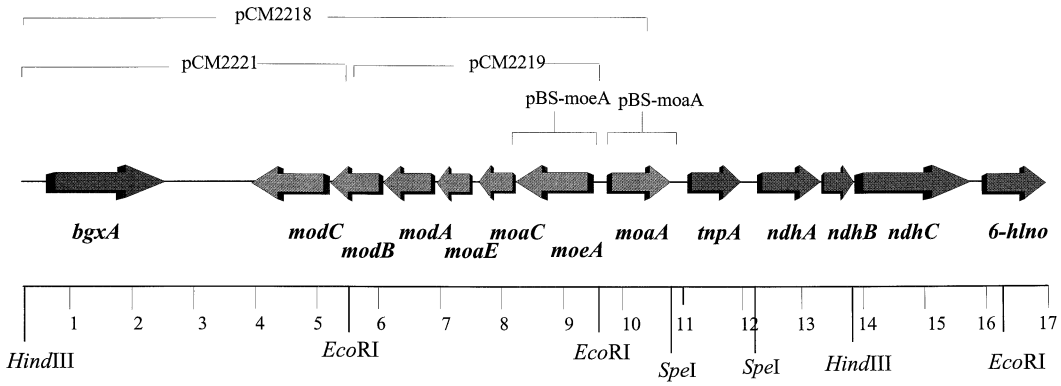

Fig. 1. Schematic representation of the arrangement of ORF on a 17-kb pAO1 DNA fragment. ORF with similarity to *mol* genes (*moaA, moeA, moaC, moaE* and *modABC*), the genes of nicotine dehydrogenase (the *ndhABC* operon), and the *6-hlno* gene are indicated. Relevant restriction sites and subclones are indicated.

intensities of the spots on the autoradiographs was determined by densitometry. ATP, GTP, CTP and UTP were used for the tests.

Anti-MoeA serum. A polyclonal antiserum against purified MoeA was raised in rabbits by standard procedures. The MoeA-specific antibodies were isolated by incubating the antiserum with nitrocellulose strips to which the purified protein was immobilized. The bound antibodies were eluted with glycine pH 2.3, immediately neutralized, and used to identify tubulin-bound MoeA.

Infrared absorbtion spectroscopy. Infrared spectra of MoeA were obtained with a Bruker IFS FTIR spectrometer equipped with an MCT detector. The spectra were recorded at a resolution of 2 cm^{-1} and apodized with a triangular function and a zero-filling factor of 2, resulting in data encoded every 1 cm^{-1}. The 2 mg/ml MoeA sample was dialyzed against water and dried on a CaF_2 window for measurements. To measure the relative areas of the amide-I components, the spectra were curve fitted by means of a least-squares iterative program (Arrondo et al., 1993)

Electron microscopy. Purified MoeA was attached to lacy carbon grids with ultrathin Formvar, stained at 4°C with 2% uranyl acetate for 3 min, and air dried. Images were taken at 100 kV with a Philips EM420 transmission electron microscope. Atomic force microscopy (AFM) of MoeA was performed with a Nanoscope IIIa from Digital Instruments. Samples consisted of MoeA at 1 ng/ml H_2O, applied to freshly cleaved mica sheet, dryed under nitrogen and analysed at ambient conditions.

Tubulin-binding assay. Neurotubulin was purified from fresh pig brain by two cycles of cold-induced disassembly and warm-induced assembly followed by cation-exchange perfusion chromatography (Fractogel EMDSO3−650 (m); Merck) on an FPLC system (Pharmacia). MoeA binding to polymerized tubulin was determined according to (Freudenreich, A. and Nick, P., unpublished results).

RESULTS

pAO1 carries a *mol*-gene cluster. The finding on pAO1 of a copy of the *moaA* gene close to the *ndh* genes (Menéndez et al., 1995) raised the possibility that additional genes involved in MoCo synthesis may be located on this catabolic plasmid. This possibility was tested by colony hybridization of pAO1 subclones in pBluescript KSII transformed into *E. coli* cells with a ^{32}P-labeled probe derived from *moaA*. The 10 722-bp DNA sequence of a *Spe*I−*Hin*dIII pAO1 DNA insert of a clone giving a positive hybridization signal (pCM2218) revealed the presence of a cluster of ORF resembling MoCo-biosynthetic genes upstream of and transcribed divergently to the *moaA* gene (Fig. 1). Sequence analysis indicated that the ORF exhibit high similarity to *moeA, moaC* and *moaE* genes of different organisms and to *modABC* genes of bacterial high-affinity Mo transporter. The ORF were designated according to the names of the *E. coli* genes to which they show similarity. An ORF with a high degree of identity (44.5%) to a *β*-glucosidase/xylosidase gene of *Erwinia chrysanthemi* (Vroemen et al., 1995) ends the 10 772-bp pAO1 DNA fragment. Situated between the *ndh* genes and the *moaA* gene is IS1473 (Menéndez et al., 1997).

Sequence characteristics of the putative pAO1 mol gene products. The consensus amino acid sequence GLPGNPVSA, corrersponding to the signature identifying MoeA-similar proteins (Prosite document 828; 1), was found between amino acid positions 328 and 333 of the putative MoeA protein. pAO1 MoeA contains the sequence L185SAGTVLGPRQL194 similar to that of the yeast *α*-ATPase sequence, L165IIGDRQTG-KTS176, and which includes the sequence signature GXXXXPR characteristic for Hsp70 and V-type and F-type ATPases. In addition, *E. coli* MoeA, and most other MoeA-similar proteins, present the sequence K283PFAF287. A search in the data base revealed that this signature is shared by protein kinases, calnexin, human centrosome autoantigen, and FtsZ. In pAO1 and *Anabena sp.* MoeA the sequence is altered to PXXVXXF and in *C. elegans* into KPXXVXXF.

The sequence alignment of pAO1 MoaC with putative MoaC proteins from other organisms revealed the amino acid motif TGVEMEAL (amino acids 114−121) as a previously undescribed signature characteristic of the MoaC proteins. MoaE represents the large subunit of the MoeB · MoaE heterodimeric converting factor (also called molybdopterin synthase) responsible in *E. coli* for the insertion of sulfur groups into precursor Z (Pitterle et al., 1993).

The deduced sequence of ModA reveals a characteristic N-terminal amino acid signal peptide (Nielsen et al., 1997), which suggests translocation of the protein through the cytoplasmic membrane. The pAO1 *modB* gene encodes a putative protein with five distinct hydrophobic regions that could serve as membrane-spanning areas. The C-terminal domain carries the consensus amino acid signature of the membrane component of the transport systems (Prosite document 364; 1). The putative *modC* product shows similarity to a long list of ATP-binding proteins belonging to the ATP-binding-cassette transport systems (Higgins, 1992).

The ORF of the pAO1 *mol* genes carried on the recombinant plasmids listed in Table 1 could be expressed in an *E. coli in*

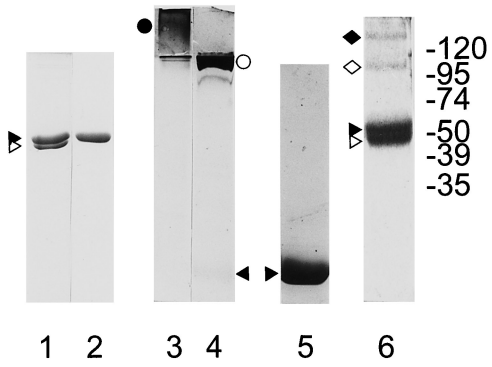

Fig. 2. Analysis of MoeA by PAGE. Lane 1, 5 μg MoeA were heated in sample buffer to 95°C for 5 min and submited to SDS/PAGE on a 12% gel. The triangles indicate the two MoeA forms. Lane 2, same MoeA preparation as in lane 1, but treated with 1% mercaptoethanol in the sample buffer. Lane 3, 10 μg MoeA analysed by native PAGE on a 5% stacking gel and 8% running gel. The closed circle indicates the position of MoeA. Lane 4, same MoeA preparation as in lane 3, but heated in SDS/PAGE sample buffer for 5 min at 95°C. The open circle indicates the position of the main MoeA band, and the triangle indicates the position of MoeA monomers. Lane 5, same MoeA preparation as in lane 3, analysed by SDS/PAGE after heating the sample in SDS/PAGE sample buffer for 5 min at 95°C. The position of MoeA monomers is indicated by a triangle. Lane 6, glutaraldehyde cross-liking products analysed by SDS/PAGE on 10% gels. Triangles indicate the positions of the two forms of MoeA monomers and diamonds indicate the positions of the glutaraldehyde cross-linking products. The molecular masses of protein markers are given in kDa.

vitro transcription/translation system into proteins of the expected sizes (results not shown).

***E. coli mol*-gene mutants are functionally complemented by pAO1 *mol* genes.** To obtain a successful complementation of *E. coli mol* mutants it was necessary to subclone each gene individually (Table 1). Using nitrate reductase as an indicator of functional MoCo synthesis, it could be demonstrated, as shown previously for *moaA* (Menéndez et al., 1995), that *moeA* and *modC* from pAO1 functionally complement mutant *E. coli* strains RK5201 (*moeA*) and RK5202 (*modC*).

Overexpression and purification of MoeA. Recombinant pAO1 MoeA was overexpressed in *E. coli* as a fusion protein with a His_6 N-terminal extention, and purified on Ni^{2+}-chelating Sepharose. When analysed by SDS/PAGE MoeA migrated as two bands (Fig. 2). Increasing the concentration of mercaptoethanol in the sample buffer resulted in the transformation of the doublet into a single band (Fig. 2). MoeA contains two cysteine residues (Cys181 and Cys336), which may form a disulfide bridge in the protein. Cys residues are present in similar positions in MoeA proteins of other origins. When analysed by native PAGE, MoeA remained in the 5% stacking gel (Fig. 2). Treatment with thrombin, which removes the His_6 extension from the fusion protein, did not change the behaviour of MoeA. MoeA apparently forms large-molecular-mass complexes. This conclusion is supported by the observation that MoeA solutions at concentrations above 1 mg/ml spontaneously form gels. The transition from sol to gel may be tested by inverting the plastic tube containing MoeA. When boiled with SDS/PAGE sample buffer and applied to the native gel, only a small proportion of the protein appeared as monomers. The main part of the protein hardly entered the 8% gel (Fig. 2). We estimate the molecular mass of these MoeA aggregates as over 200 kDa when compared with the migration of the 205-kDa rabbit muscle myosin (results not shown). It required boiling in SDS/PAGE sample buffer and submission to SDS/PAGE to release MoeA monomers (Fig. 2). Cross-linking with glutaraldehyde and analysis of the cross-linked products by SDS/PAGE revealed the formation of MoeA dimers and trimers (Fig. 2).

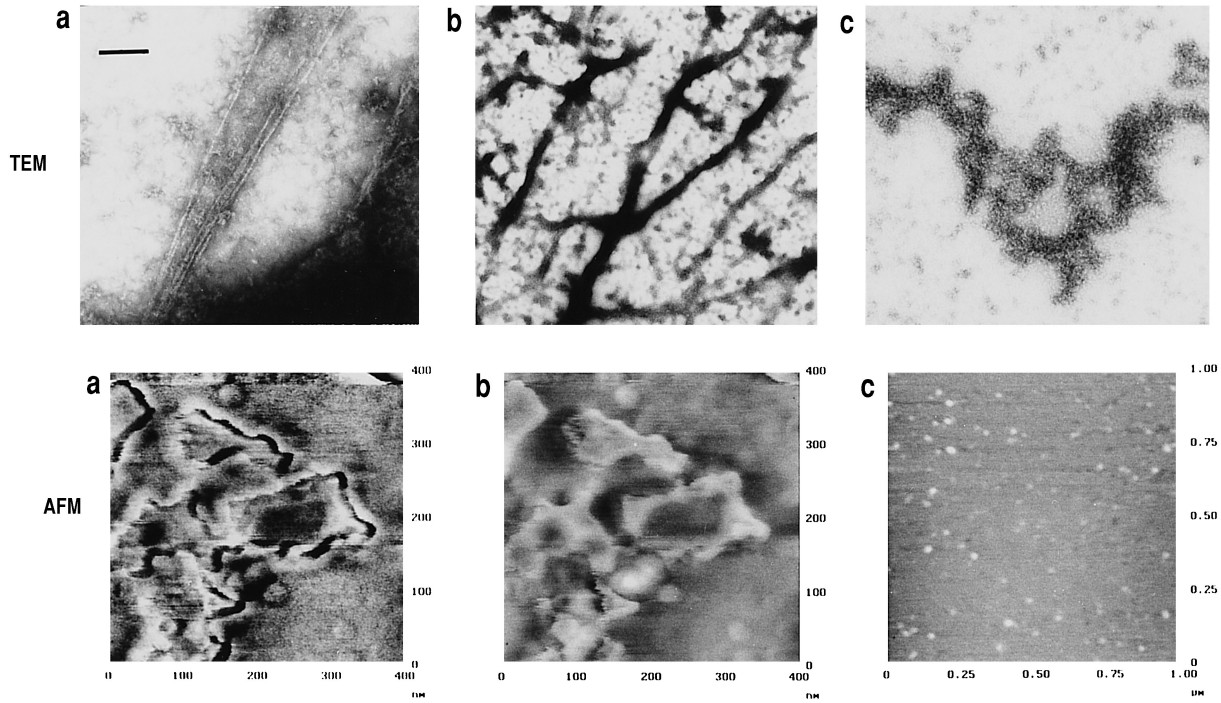

Fig. 3. TEM and AFM images of MoeA. Samples of 1.6 mg/ml MoeA were prepared for TEM as indicated in Materials and Methods. (a) MoeA fibres; (b) network of MoeA fibres formed at pH 11 by addition of KOH to the MoeA sample; (c) desaggregation of MoeA fibres to more amorphous aggregates in the presence of ATP and Mg^{2+}. The black bar in (a) represents 3 μm. MoeA samples were prepared for AFM as indicated in Materials and Methods and recorded in tapping mode. (a) MoeA, phase image; (b) MoeA, high image; (c) BSA, high image.

Electron microscopy reveals MoeA fibers. The high molecular mass of native MoeA prompted us to analyse its appearance in the electron microscope. Transmission electron microscopy (TEM) showed the presence in the MoeA preparation of long fibres, approximately 10−30 nm wide (Fig. 3). Adjustment of the pH of the MoeA preparation with KOH to pH 11 increased the tendency of MoeA to form a gel. Viewed in the TEM the preparation showed a network of fibers (Fig. 3). The presence of fibers was characteristic for MoeA preparations and did not occur with other protein preparations, e.g. BSA and mitochondrial F_1-ATPase (results not shown). MoeA appeared as fibrous structures in the AFM (Fig. 3). Fibres did not occur with BSA (Fig. 3).

MoeA exhibits an average distribution of secondary-structure elements. The formation of fibers may suggest that the protein adopts a predominant type of secondary structure. Infrared spectroscopy, however, indicated a secondary-structure composition of 32.2% β-sheet, 29.7% random, 29.7% α-helix and 11.9% turn.

MoeA exhibits ATPase activity. The nucleotide motifs identified in the amino acid sequence of MoeA suggested a nucleotide hydrolytic activity of the protein. Incubation of [^{32}P]ATP with MoeA generated ADP. The reaction was temperature dependent (Fig. 4A) and required Mg^{2+} (Fig. 4A). GTP was not hydrolysed (Fig. 4A), nor was CTP, TTP or UTP (results not shown). The ADP formed in the *in vitro* reaction was transformed within 24 h mostly into AMP (Fig. 4A). Addition of mercaptoethanol to the assay inhibited the ATPase activity (Fig. 4A). Apparently, the proposed disulfide bridge of the protein was needed to keep the protein in an active form. The time-dependent and protein-concentration-dependent hydrolytic activity of MoeA is presented in Fig. 4B. A rate of 0.02 pmol ATP hydrolysed · pmol MoeA^{-1} · min^{-1} was calculated. This rate is comparable to that exhibited by weak ATPases, such as DnaK (McCarty et al., 1995).

Since MoeA exhibits some sequence similarity to Ca^{2+}-dependent ATPases and since it is involved in the synthesis of the molybdenum-containing cofactor we tested the effect of Ca^{2+} and MoO_4^{2-} on the ATPase activity of MoeA. When these ions were added instead of Mg^{2+} to the reactions no ATP hydrolytic activity of MoeA could be detected (results not shown). In the presence of Mg^{2+}, Ca^{2+} inhibited the reaction, but molybdate enhanced the reaction rate in a concentration-dependent manner (Fig. 4C).

The standard reaction buffer was 10 mM Tris/HCl, pH 7.5, 10 mM $MgCl_2$. A 2−3-fold increase in reaction rate was observed for the same MoeA preparation in 10 mM Tris/acetate, pH 7.5, 10 mM Mg acetate, 50 mM K acetate and 0.5 mM dithioerythritol. The reaction rate was decreased approximately fivefold in 50 mM Tris/HCl, pH 7.5, 10 mM $MgCl_2$ and 100 mM NaCl. The ATPase activity was associated with the high-molecular-mass form of MoeA as could be demonstrated by incubating the MoeA trapped in the 5% stacking gel afternative PAGE with [α-^{32}P]ATP (results not shown). Control reactions with stacking gel alone gave no ATP hydrolysis. During the first hours of the reaction only ADP, and no AMP, was detected. The very slow turnover of ADP into AMP may reflect a low hydrolytic activity of MoeA with ADP as substrate. We consider the presence of traces of a contaminating nucleotide pyrophosphatase as unlikely. When [γ-^{32}P]ATP was used in the assay MoeA was not phosphorylated.

MoeA changes conformation in the presence of nucleotides. TEM images of MoeA incubated with ATP in the presence of

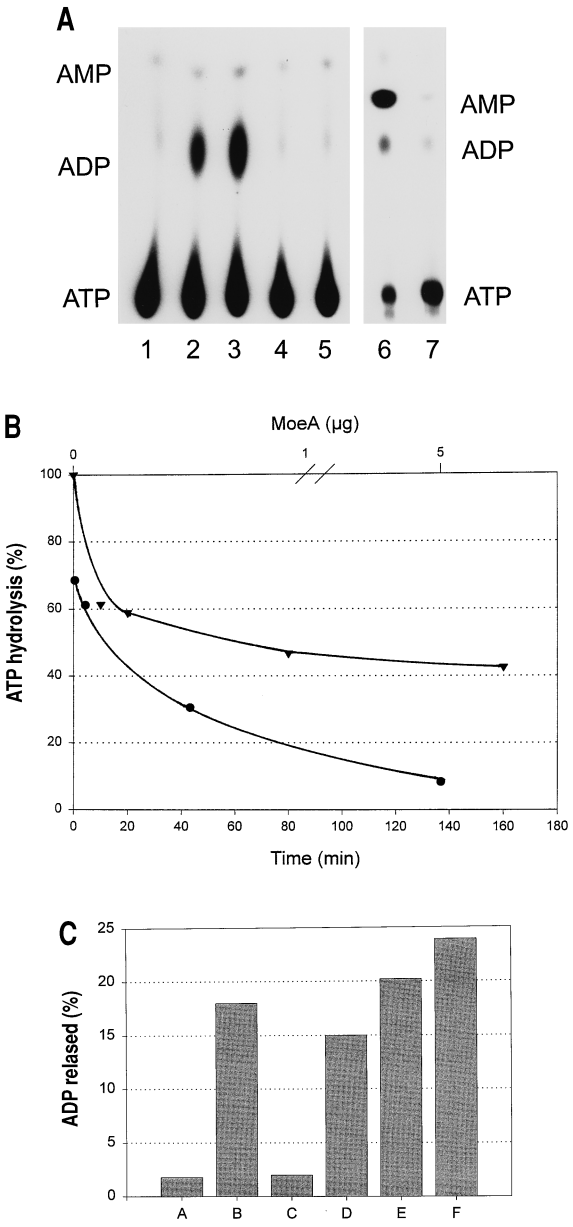

Fig. 4. ATPase activity of MoeA. (A) MoeA-dependent [α-^{32}P]ATP hydrolysis was monitored on thin-layer plates as described in Material and Methods. Lane 1, control sample without MoeA; lane 2, 60 min incubation with 0.5 µg MoeA at 30 °C; lane 3, 60 min incubation with 0.5 µg MoeA at 37 °C; lane 4, 60 min incubation with 0.5 µg MoeA at 30 °C in the absence of Mg^{2+}; lane 5, 60 min incubation of [α-^{32}P]GTP with 0.5 µg MoeA at 30 °C; lane 6, 24 h incubation with MoeA at 30 °C; lane 7, 24 h incubation with MoeA at 30 °C in the presence of 1% mercaptoethanol. (B) Time-dependent and MoeA-concentration-dependent ATP hydrolysis. [^{32}P]ATP was incubated with 1 µg ATP under standard assay conditions for the times indicated, and the amount of ATP (▼) in the sample was determined following autoradiography of the TLC plate and quantification by densitometry of the intensity of the spot corresponding to ATP. For the determination of the MoeA-concentration-dependent ATP hydrolysis (●), standard assays were incubated at 30 °C for 60 min in the presence of 0.1, 1 and 5 µg MoeA, separated by TLC, the thin-layer plate autoradiographed, the autoradiographic spots quantified by densitometry and the intensities expressed as percentages of those obtained for ATP in the absence of MoeA. (C) Effect of Ca^{2+} and MoO_4^{2-} on the ATPase activity of MoeA expressed as a percentage of the ADP released. Standard assays were performed with 1 µg MoeA in the absence of 1 mM Mg^{2+} (A), or in the presence of 1 mM Mg^{2+} (B), 1 mM Mg^{2+} and 1 mM Ca^{2+} (C), 1 mM Mg^{2+} and 0.1 mM MoO_4^{2-} (D), 1 mM Mg^{2+} and 1 mM MoO_4^{2-} (E) or 1 mM Mg^{2+} and 10 mM MoO_4^{2-} (F).

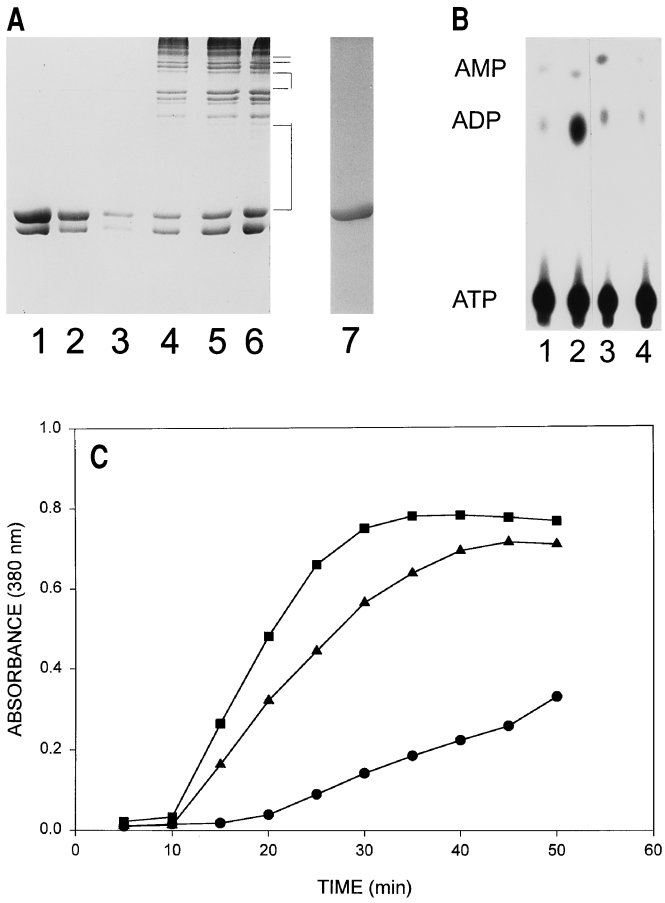

Fig. 5. Aggregation of MoeA in the presence of nucleotides. (A) Analysis by SDS/PAGE on 8% gels of MoeA in the supernatant (lanes 1−3) and pellet (lanes 4−6) obtained by centrifugation of 20 µl samples taken at 20, 40 and 60 min, respectively, from a 1 mg/ml MoeA solution incubated with 1 mM ATP and 1 mM Mg^{2+}. Lines on the right side of lane 6 indicate discrete multimeric forms of MoeA. The supernatant and pellet samples were mixed with 10 µl denaturing sample buffer, heated for 2 min at 95 °C and submitted to SDS/PAGE. Lane 7, a pellet sample was heated for 10 min at 95 °C in denaturing sample buffer with 1% mercaptoethanol. (B) [α-^{32}P]ATPase activity of supernatant and pellet obtained by centrifugation of a 1 mg/ml MoeA sample incubated for 60 min at 30 °C with 1 mM ATP and 1 mM Mg^{2+}. Lane 1, control without MoeA; lane 2, 0.5 µg MoeA in 20 µl standard assay in the presence of Mg^{2+}; lane 3, activity of supernatant fraction; lane 4, activity of pellet fraction. (C) Formation of MoeA aggregates measured by the increase in absorbance at 380 nm in the presence of 1 mM Mg^{2+} only (●), in the presence of ATP, ADP or AMP (▲), or in the presence of ATP and Mg^{2+} (■).

Mg^{2+} showed that the fibres are replaced by a more amorphous, aggregated form of MoeA (Fig. 3). MoeA gels formed at 2 mg/ml in the elution buffer of the Ni^{2+}-chelate-affinity chromatography were immediately transformed into sol upon addition of 1 mM ATP and 1 mM Mg^{2+} to the sample. This change was associated with the formation of MoeA aggregates as demonstrated by SDS/PAGE. Fig. 5 shows the analysis of samples taken at increasing times after addition of Mg^{2+} · ATP to the MoeA sample. At 20, 40 and 60 min aliquots of the reaction assay were centrifuged. The supernatants and the pellets were incubated for 2 min at 95 °C in SDS/PAGE sample buffer and applied to SDS/PAGE on an 8% gel. An increasing depletion of MoeA from the supernatant was observed (Fig. 5A). MoeA appeared in its two monomeric forms, probably according to whether the disulfide bridge in the protein was reduced or not. Only a few faint bands of MoeA oligomers were present. The pellet of MoeA aggregates was resolved on the denaturing gel, in addition into the monomeric forms, into discrete multimeric forms (Fig. 5A). Apparently, in the presence of ATP · Mg^{2+} there is a tight association of MoeA subunits. The subunits were not covalently bound to each other, since incubation in SDS/PAGE sample buffer for 10 min at 95 °C led to the dissociation of the multimers into the monomeric form (Fig. 5A).

The ATPase activity disappeared after centrifugation from the supernatant of the MoeA samples incubated with Mg^{2+}-ATP (Fig. 5B). The MoeA aggregates recovered in the pellet did not redissolve in the assay buffer and showed no ATPase activity (Fig. 5B). The transition of MoeA from the soluble to the aggregated state can be followed by measuring the increase in absorbance at 380 nm. When a 0.1 mg/ml solution of MoeA was incubated in the presence of Mg^{2+} a slight, but steady, increase in absorption was observed (Fig. 5C). Addition of ATP, ADP or AMP in the absence of Mg^{2+} resulted in an accelerated increase in absorbance, which leveled off within 50 min (Fig. 5C). When ATP was added in the presence of Mg^{2+} the increase in absorption was more rapid and reached its maximum within 30 min (Fig. 5C). Apparently, nucleotides in the absence of Mg^{2+} ions can induce the transition to MoeA aggregates. However, ATP hydrolysis accelerated this process.

MoeA binds neurotubulin dimers. The amino acid sequence of pAO1 MoeA shows 39% identity to the C-terminal part of gephyrin, which is the neurotubulin-binding part of this protein (Prior et al., 1992). The similarity in sequence is reflected in a functional similarity since MoeA showed affinity to neurotubulin, particularly to the non-polymerized dimeric form (results not shown).

DISCUSSION

One unexpected finding of the present work is that genes of MoCo biosynthetic enzymes and of a high-affinity Mo ATP-binding-cassette transporter are located on the catabolic plasmid pAO1 next to MoCo-dependent-enzyme genes required for nicotine catabolism. Results showing that the expression of the pAO1 *mol* genes is induced by nicotine support the assumption that the nicotine dehydrogenase genes and those of Mo uptake and MoCo synthesis form a regulatory and functional unit on pAO1. The clustering of *mol* genes on pAO1 may reflect a selective pressure on the plasmid genome during its evolution. The increased level of MoCo-enzyme synthesis in the presence of nicotine must be coordinated with the level of MoCo synthesis to form functionally active holoenzymes. The increased demand for MoCo may not be met by the constitutive expression of the chromosomally encoded genes and therefore may require the coexpression of the plasmid genes. The presence of IS1473 (Menéndez et al., 1997) between the *ndh* genes and the MoCo-synthesis and Mo-transporter gene cluster may indicate that this arrangement resulted from a translocation event.

The ATP-binding-cassette Mo transporter of pAO1 presents only one membrane-spanning-protein gene (*modB*) in agreement with other ATP-binding-cassette Mo transporters (Johann and Hinton, 1987; Luque et al., 1993; Wang et al., 1993). It is proposed that the pore for MoO_4^{2-} translocation is formed by a homodimer of ModB, which presents five membrane-spanning domains/subunit (Maupin-Furlow et al., 1995). Each transporter system has two ATP-binding domains, which in many cases are identical and coded by the same gene (Higgins, 1992). This

seems to be the situation in the *A. nicotinovorans* pAO1 system since no other ORF displaying ATPase motifs was found on the pCM2218 insert. The complementation of the *E. coli modC* mutant by the *Arthrobacter* pAO1 *modC* gene indicates a functionally correct interaction of ModB and ModC in these two organisms.

The *moaA*, *moeA*, *moaC* and *moaE* gene products may be responsible for essential steps in MoCo biosynthesis and were therefore acquired with the Mo transporter by the plasmid. Of the gene products encoded by the pAO1 *mol* genes, only the function of MoaE, which with MoaD forms the molybdopterin synthase, is known. The high degreee of evolutionary conservation of MoeA throughout all kingdoms of life is remarkable. In mammals the C-terminal part of the two-domain protein gephyrin, which is similar to MoeA, is responsible for the anchorage and positioning of the β subunit of the glycin receptor to the tubulin cytoskeleton of spinal cord neurons. A structural function of MoeA is suggested by *in vitro* analysis of its properties. The MoeA gel is formed by a network of MoeA fibers as shown in the TEM. According to the glutaraldehyde cross-linking data the basic subunits appear to represent MoeA dimers and/or trimers. Similarly to other cytoskeleton proteins, MoeA exhibits nucleotidase activity and changes its aggregation state in the presence of nucleotides. The change in structure apparently does not require ATP hydrolysis since it can be induced by ATP, ADP or AMP in the absence of Mg^{2+}, an observation also made recently with the chaperonin heat-shock protein 60 of *Sulfolobus shibatae* (Trent et al., 1997). A hint for a structural function of the protein may come from its sequence similarities to *E. coli* FtsZ and the affinity for tubulin. The higher affinity to depolimerized tubulin may reflect the interaction of tubulin dimers with the MoeA fibers. Attempts to establish an interaction between MoeA and FtsZ *in vitro* were non-conclusive. Efforts will have to be undertaken to establish the structural features *in vivo* of MoeA and its intracellular protein partners.

How may the characteristics of MoeA relate to its function in MoCo synthesis? We propose that MoeA plays the role of a scaffold on which the last steps in the synthesis of MoCo take place. Its assembly appears regulated by ATP hydrolysis, Ca^{2+} and the presence of MoO_4^{2-}. The molybdate taken up by the bacterium has to be protected from unspecific interactions with cellular components and directed to the specific insertion into the precursor Z. MoeA may yield the structural frame for the interaction with the molybdate-uptake system, the channelling of the metal to the organic moiety of the cofactor and the interaction with additional protein factors involved in MoCo synthesis. As suggested for gephyrin (Prior et al., 1992; Kirsch et al., 1993), MoeA could be more generally involved in regulating the cell-surface distribution of ion-channel proteins.

We thank Dr V. Stewart for providing the *E. coli* mutant strains, Prof. Dr P. Gräbner for support with infrared spectroscopy and Mr W. Fritz for help with the illustrations. This work was supported by a grant form the *Deutsche Forschungsgemeinschaft* to R. B.

REFERENCES

Arrondo, J. L. R., Muga, A., Castesana, J. & Goni, F. M. (1993) Quantitative studies of the structure of proteins in solution by Fourier transform infrared spectroscopy, *Prog. Biophys. Molec. Biol. 59*, 23−56.

Bairoch A., Bucher, P. & Hofmann, K. (1995) The PROSITE database, its status in 1995, *Nucleic Acids Res. 24*, 189−196.

Bernauer, H., Mauch, L. & Brandsch, R. (1992) Interaction of the regulatory protein NicR1 with the promoter region of the pAO1-encoded 6-hydroxy-D-nicotine oxidase gene of *Arthrobacter oxidans*, *Mol. Microbiol. 6*, 1809−1820.

Berthold, H., Scanarini, M., Abney, C. C., Frorath, B. & Northemann, W. (1992) Purification of recombinant antigenic epitopes o the human 68-kDa (U1) ribonucleoprotein antigen using the expression system pH6EX3 followed by metal chelating affinity chromatography, *Protein Expr. Purif. 3*, 50−56.

Eberwein, H., Gries, F. A. & Decker, K. (1961) I. Über den Abbau des Nicotins durch Bakterienenzyme. II. Isolierung und Charakterisierung eines Nicotinabbauenden Bodenbakteriums, *Hoppe-Seyler's Z. Physiol. Chem. 323*, 236−48.

Gonnet, G. H., Cohen, M. A. & Benner, S. A. (1992) Exhaustive matching of the entire protein sequence database, *Science 256*, 1443−1445.

Grether-Beck, S., Igloi, G. L., Pust, S., Schilz, E., Decker, K. & Brandsch, R. (1994) Structural analysis and molybdenum-dependent expression of the pAO1-encoded nicotine dehydrogenase genes of *Arthrobacter nicotinovorans*, *Mol. Microbiol 13*, 929−936.

Higgins, C. F. (1992) ABC transporters: from microorganisms to man, *Annu. Rev. Cell Biol. 8*, 67−113.

Kamdar, K. P., Shelton, M. E. & Finnerty, V. (1994) The *Drosophila* molybdenum cofactor gene cinnamon is homologous to three *Escherichia coli* cofactor proteins and to the rat protein gephyrin, *Genetics 137*, 791−801.

Kirsch, J., Wolters, I., Triller, A. & Betz, H. (1993) Gephyrin antisense oligonucleotides prevent glycine receptor clustering in spinal neurons, *Nature 366*, 745−748.

Kretzer, A., Fruntzke, K. & Andreesen, J. R. (1993) Catabolism of isonicotinate by *Mycobacterium sp.* INA1: extended description of the pathway and purification of the molybdoenzyme isonicotinate dehydrogenase, *J. Gen. Microbiol. 139*, 2763−2772.

Luque, F., Mitchenall, L. A., Chapman, M., Christine, R. & Pau, R. N. (1993) Characterization of genes involved in molybdenum transport in *Azotobacter vinelandii*, *Mol. Microbiol. 7*, 447−459.

Maupin-Furlow, J. A., Rosentel, J. K., Lee, J. H., Deppenmeier, U., Gunsalus, R. P. & Shanmugam, K. T. (1995) Genetic analysis of the *modABCD* (molybdate transport) operon of *Escherichia coli*, *J. Bacteriol. 177*, 4851−4856.

McCarty, J. S., Buchberger, A., Reinstein, J. & Bukau, B. (1995) The role of ATP in the functional cycle of the DnaK chaperone system, *J. Mol. Biol. 249*, 126−137.

Menéndez, C., Igloi, G. L. & Brandsch, R. (1997) IS1473, a putative insertion sequence identified in the plasmid pAO1 from *Arthrobacter nicotinovorans*: isolation, characterization and distribution among *Arthrobacter* species, *Plasmid 37*, 35−41.

Menéndez, C., Henninger, H. & Brandsch, R. (1995) A pAO1-encoded molybdopterin cofactor gene (*moaA*) of *Arthrobacter nicotinovorans*: characterization and site-directed mutagenesis of the encoded protein, *Arch. Microbiol. 164*, 142−151.

Menéndez, C., Siebert, D. & Brandsch, R. (1996) MoaA of *Arthrobacter nicotinovorans* pAO1 involved in Mo-pterin cofactor biosynthesis is an Fe-S protein, *FEBS Lett. 391*, 101−103.

Nielsen, H., Engelbrecht, J., Brunak, S. & von Heijne, G. (1997) Identification of prokaryotic and eukaryotic signal peptides and prediction of their cleavage sites, *Protein Eng. 10*, 1−6.

Pitterle, D. M., Johnson, J. L. & Rajagopalan, K. V. (1993) *In vitro* synthesis of molybdopterin from precursor Z using purified converting factor, *J. Biol. Chem. 268*, 13506−13509.

Prior, P., Schmitt, B., Grenningloh, G., Pribila, G., Multhaup, G., Beyreuther, K., Maulet, Y., Werner, P., Langosch, D., Kirsch, J. & Betz, H. (1992) Primary structure and alternative splice variants of gephyrin, a putative glycine receptor-tubulin linker protein, *Neuron 8*, 1161−1170.

Rajagopalan, K. V. & Johnson, J. L. (1992) The pterin molybdenum cofactors, *J. Biol. Chem. 267*, 10199−10202.

Sambrook, J., Fritsch, E. F. & Maniatis, T. (1989) Molecular cloning: a laboratory manual, 2nd edn, Cold Spring Harbor Laboratory, Cold Spring Harbor NY.

Stewart, V. & MacGregor, C. H. (1982) Nitrate reductase in *Escherichia coli* K-12: role of *chlC*, *chlE*, and *chlG* loci, *J. Bacteriol. 151*, 788−799.

Trent, J. D., Kagawa, H. K., Yaoi, T., Olle, E. & Zaluzec, N. J. (1997) Chaperon filaments: the archael cytoskeleton? *Proc. Natl Acad. Sci. USA 94*, 5383−5388.

Vroemen, S., Heldens, J., Boyd, C., Henrissat, B. & Keen, N. T. (1995) Cloning and characterization of the *bgxA* gene from *Erwinia chrysanthemi* D1 which encodes a *β*-glucosidase/xylosidase enzyme, *Mol. Gen. Genet. 246*, 465−477.

Wang, G., Angermüller, S. & Klipp, W. (1993) Characterization of *Rhodobacter capsulatus* genes encoding a molybdenum transport system and putative molybdenum-pterin-binding proteins, *J. Bacteriol. 175*, 3031−3042.

Worley, K. C., Wiese, B. A. & Smith, R. F. (1995) BEAUTY: an enhanced BLAST-based search tool that integrates multiple biological information resources into sequence similarity search results, *Genome Res. 5*, 173−184.

Yanish-Perron, C., Viera, J. & Messing, J. (1985) Improved M13 phage cloning vectors and host strains: nucleotide sequence of the M13mp18 and pUC19 vectors, *Gene* (*Amst.*) *33*, 103−119.